2016

Effect of Inclination on Pressure Drop in Large Flattened-Tube Steam Condensers

Yu Kang
ACRC, University of Illinois, United States of America, yukang2@illinois.edu

William A. Davies
ACRC, University of Illinois, United States of America, daviesi2@illinois.edu

Pega Hrnjak
pega@illinois.edu

Anthony M. Jacobi
ACRC, University of Illinois, United States of America, a-jacobi@illinois.edu

Effect of Inclination on Pressure Drop in Large Flattened-Tube Steam Condensers

Yu Kang[1], William A. Davies[1], Pega Hrnjak[1,2]*, Anthony M. Jacobi[1]

[1]Air Conditioning and Refrigeration Center (ACRC), Department of Mechanical Science and Engineering,
University of Illinois at Urbana-Champaign,
Urbana, IL, USA
yukang2@illinois.edu, daviesi2@illinois.edu, pega@illinois.edu, a-jacobi@illinois.edu

[2]CTS – Creative Thermal Solution, Inc.
Urbana, IL, USA

* Corresponding Author

ABSTRACT

This paper presents the experimental study of the inclination effect on condensation pressure drop in a large-scale flattened tube used in an Air-Cooled Condenser (ACC) for steam. Slightly-superheated steam with mass flux of 6.8 kg m^{-2} s^{-1} was condensed inside a 10.7 m long, flattened half-tube with inclination angle varied from horizontal to 13.2˚. A uniform velocity profile of 2.03 ± 0.12 m s^{-1} was imposed on the air side to extract heat from the steam. Initial two-phase pressure drop measurements and flow visualization showed a reduction of pressure drop due to improvement in the gravity-assisted drainage of condensate inside the tube, although improvement was only seen at an early stage of inclination. To create a visualization window, the tube was cut in half, and thus a model that accounts for the differences in tube material and size between the real, full, flattened condenser tube and test tube was developed and validated in the single-phase flow scenario. This model enables the prediction of pressure drop under different inclination configurations in the actual ACC in power plants by using the experimental results obtained in this study. Heat transfer results are presented in a companion paper.

1. INTRODUCTION

In the application of condenser tubes for refrigeration, nuclear and thermal power generation industries, the characteristics of pressure drop are of great importance for system design and optimization. Multiple factors, such as tube geometry, local vapor quality, mass flux and tube inclination, influence the flow pattern, and thus heat transfer and pressure drop, in a convoluted manner. A large number of correlations for two-phase pressure drop have been developed based on experimental investigations. Coleman & Garimella (2003) studied two-phase flow regimes in round, square and rectangular tubes during condensation of R134a. Their results showed that flow regime transitions are not very strongly dependent on tube shape and aspect ratio for similar hydraulic diameters. Pressure drop correlations for two-phase flow in horizontal rectangular channels were also described by Wambsganss et al (1992) and Lee & Lee (2001). The modification of parameter C in the Lockhart-Martinelli correlation improved pressure drop predictions when the effect of small gap size needs to be taken into account. Kim et al (2013) reasonably predicted the pressure drop during the condensation of R410a using the Muller-Steinhagen and Heck correlation with hydraulic diameter or Friedel correlation with equivalent diameter. In addition to the tube shape, flow patterns are influenced by the tube inclination, but few studies are available to investigate the effect of tilting angle on heat transfer and pressure drop during condensation (Lips & Meyer, 2011). Two-phase frictional pressure drop in rectangular channels studied by Ide & Matsumura (1990) proved that Lockhart-Martinelli correlation and Akagawa's correlation do not agree well with the experimental data when inclination angle is large and superficial liquid velocity is small. A more comprehensive study done by Lips & Meyer (2012) provided detailed results of pressure drop during the condensation of R134a in a round tube for a whole range of inclination angles. The concept of apparent gravitational pressure drop and apparent void fraction were intruduced to quantify the effect of inclination on the flow. Groenewald & Kroger (1995) quantified the effect of mass transfer on wall friction for turbulent steam vapor flow inside ducts during condensation. Their correlations on numerical integration of the vapor velocity profile agreed well with experimental data within ± 5% error. These studies confirmed and quantified the effect of tube geometry and inclination angle on condensation pressure drop, but pressure drop models for a large-scale flattened tube with low mass flux are not available and thus need to be developed.

In order to address these issues, an experimental facility was designed and built to test a condenser tube in the same scale as those used in power plants. Measurements were taken of heat transfer and pressure drop at different inclination angles during the condensation of steam. To observe flow patterns, the flattened tube was cut in half and a polycarbonate window replaced the removed part, forming a half-tube test section. Such a half-tube design complicated the interpretation of the pressure drop tests by removing the direct applicability of the measurements to pressure drop in an actual power-plant condenser tube. However, such a sacrifice was paid off by having clear visual access to the flow regimes along the entire length of the condenser tube and at different inclination angles. Flow patterns, and their alteration with inclination angle, have a strong influence on the two-phase pressure drop, therefore it is essential to work with such a design. Nonetheless, special attention must be paid to accurately predicting the pressure-drop performance of the actual condenser tube, and therefore a model to relate the pressure drop measurement in the test tube to full tubes was developed.

2. EXPERIMENT DESCRIPTION

2.1 Experiment Facility

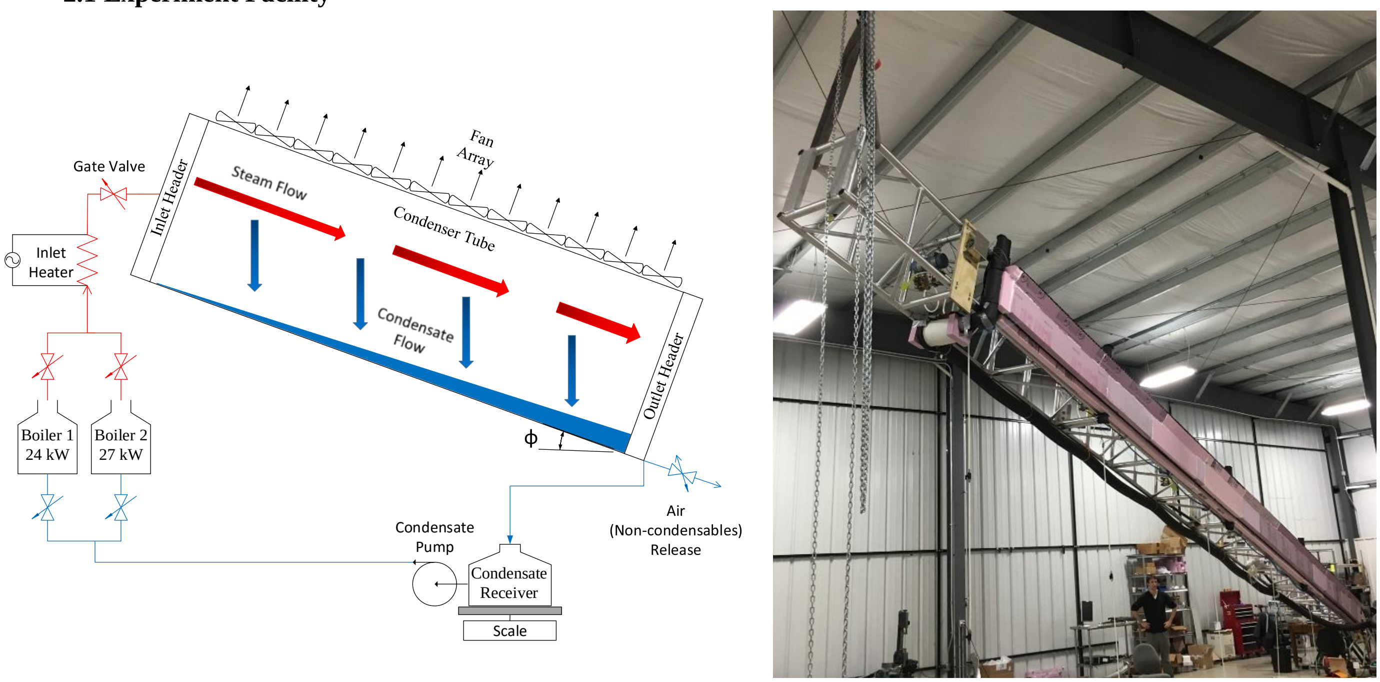

(a) (b)

Figure 1: Experimental Facility: (a) Schematic Drawing, (b) Actual Facility

The experiment facility is shown in Figure 1. The cross-sectional area of the flattened condenser test tube in this study is half of the full tubes widely used in ACC power plants. Typical dimensions of the full tube are 10.7 m in length, 0.214 m in height and 0.02 m in width as is shown in Figure 2. After cutting the original full tube into half and adding the polycarbonate window, a test tube with one side transparent was assembled and is shown in Figure 3.

On the steam side, two boilers running in parallel provide a maximum power of 51 kW in steam generation, and their powers are individually controlled so that the mass flux of steam can be properly varied. A pipe heater is attached to the steam inlet to create superheat. Slightly-superheated steam is then condensed inside the test tube. Foam insulation is attached to the polycarbonate window so that an adiabatic condition on the polycarbonate side can be maintained when not doing visualization. To study the effect of inclination on pressure drop and heat transfer, the tube is able to be tilted from horizontal to vertical. At the tube exit condensate is collected in a receiver, and its mass flow rate is determined by measuring its weight change against time. A high-temperature condensate pump feeds condensate back into the two boilers intermittently, forming a semi-closed system on the steam side.

On the air side, 134 axial fans are powered to pull air upwards passing through the aluminum fins that were brazed on the condenser tube. Air flow is constrained inside an air duct with insulation on the outside to minimize heat losses. Each fan is controlled individually by a potentiometer to simulate different air flow profiles and mimic the actual operation of the condenser in power plants. A cross-sectional view of the complete assembly of the condenser tube is shown in Figure 3.

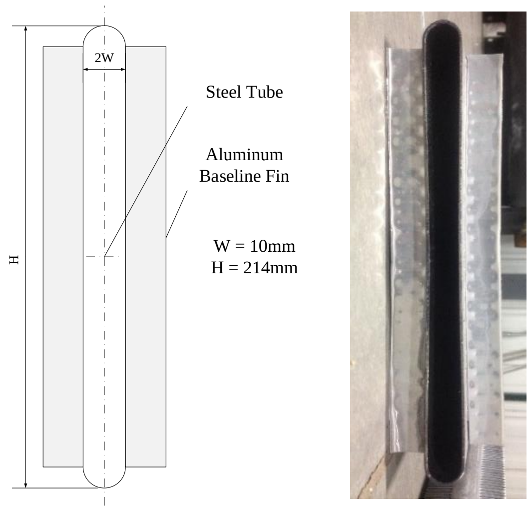

(a) (b)

Figure 2: Cross-sectional View of Full Flattened Tube: (a) Schematic, (b) Actual Photo

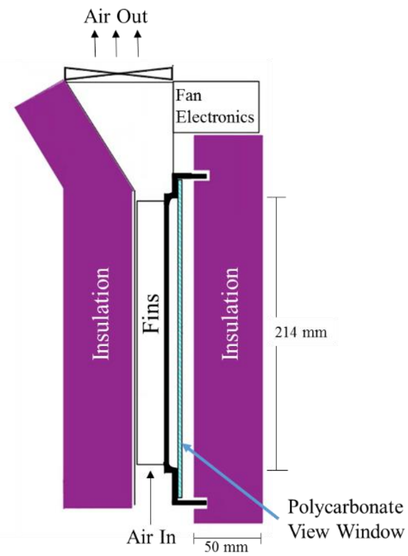

Figure 3: Cross-sectional View of the Half Flattened Tube Assembly

2.2 Measurements Points

Along the tube length, 12 sets of temperature measurements and six pressure measurement points are employed to determine the heat transfer and pressure drop on steam side. As is shown in Figure 4, five Rosemount® differential pressure transducers measure pressure drop between each adjacent pressure measurement point. The full range of the sensors are 2 inH_2O (497.68 Pa), 1 inH_2O (248.84 Pa), 1 inH_2O (248.84 Pa), 0.5 inH_2O (124.42 Pa), and 0.35 inH_2O (87.097 Pa), respectively for dP1 to dP5. The steam vapor velocity decreases from 11 m s^{-1} at the inlet to 0 at the outlet, so the sensors with larger range are selected closer to the inlet and smaller ones near the outlet. The total pressure drop in the entire tube is then obtained by adding all the individual values together. Another transducer, P_i, with range of 30 inH_2O (7465.20 Pa) is added at the inlet which measures the inlet gauge pressure to determine the inlet superheat. All these instruments have an error of 0.15% of their full range according to the instrument manual.

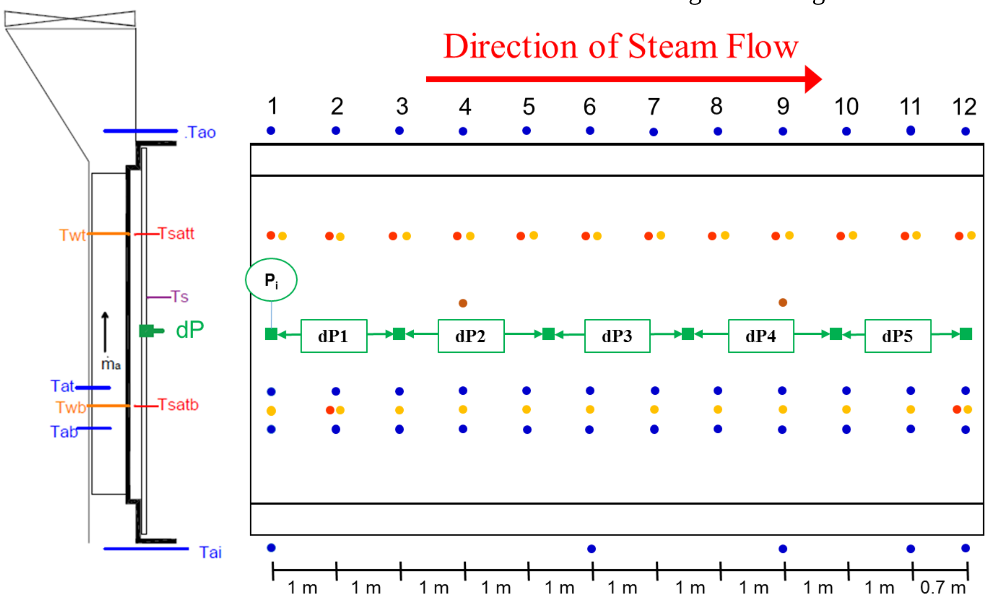

Figure 4: Measurement Points Arrangement

3. RELATING PRESSURE DROP IN TEST TUBE TO THE REAL FULL SIZE TUBE

3.1 Problem Description

The visualization access results in an artificial tube that is half-size compared to the original tube and is made of two distinct materials, steel and polycarbonate. Such differences, as is illustrated in Figure 5, complicate the process of directly comparing pressure drop in the real, full-size tubes in power plants to the experimental results from this facility. For instance, the smooth polycarbonate surface creates less frictional pressure drop than the rough steel surface in both single- and two-phase tests. Even more distinctively, no condensate is formed on the polycarbonate window in the two-phase test due to the adiabatic condition along the insulated polycarbonate, as shown in Figure 3. In contract, on the steel surface condensate is formed and generates shear stresses on the flowing steam vapor. Finally, the difference in cross-sectional area itself leads to a difference in the area/volume ratio and therefore a difference in pressure drop. Therefore, a model to relate pressure drop in the test tube to the real full size tube is needed, and this model can enable the quantification of the above-mentioned differences.

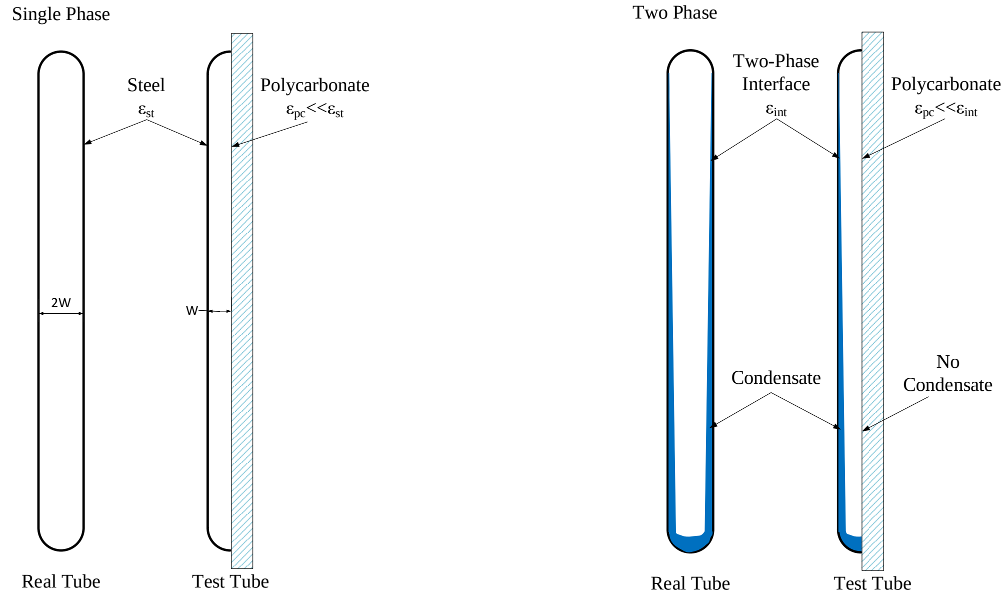

(a) (b)

Figure 5: Difference of Pressure Drop for Real and Test Tube in (a) Single Phase Test, (b) Two Phase Test

3.2 Model Description

The model for single phase uses an equivalent friction factor f_e in Equation (1) derived from the measured pressure drop of flows, ΔP, in the test tube. f_e can be expressed in terms of f_{st} and f_{pc} in Equation (2), which are calculated friction factors for hypothetical tubes made of one pure material indicated by the subscript. In Equation (2), weights, ω_{st} and $1-\omega_{st}$, are assigned to each individual friction factor based on the half-tube geometry. The weight ω_{st} is evaluated in Equation (3) according to the ratio of the circumferential length of steel L_{st} over the perimeter of the cross section. In this study, $\omega_{st} = 0.5091$ and $1-\omega_{st} = 0.4909$.

$$\Delta P = f_e \frac{L}{D_h} \frac{1}{2} \rho V^2 \tag{1}$$

$$f_e = \omega_{st} f_{st} + (1-\omega_{st}) f_{pc} \tag{2}$$

$$\omega_{st} = \frac{L_{st}}{p_{half}} = \frac{L_{st}}{L_{st}+H} \tag{3}$$

Once f_{st} is determined for the half tube, steel surface roughness can be calculated using Churchill's (1977) correlation as is shown in Equation (4):

$$f = 8\left(\left(\frac{8}{\mathrm{Re}_{D_h}} \right)^{12} + \left(A_{CH} + B_{CH} \right)^{-3/2} \right)^{1/12}, \text{ where } A_{CH} = \left(2.457 \ln \left[\left(\left(\frac{7}{\mathrm{Re}_{D_h}} \right)^{0.9} + 0.27 \frac{\varepsilon}{D_h} \right)^{-1} \right] \right)^{16}, \; B_{CH} = \left(\frac{37530}{\mathrm{Re}_{D_h}} \right)^{16} \quad (4)$$

Finally, the full-tube friction factor and pressure drop can be calculated using the same correlation and roughness as the half tube, and updating the dimensions and Reynolds number for a full tube.

This model was developed and validated for single phase, as elaborated in section 3.3. However, the same logic can be also applied to relate two-phase pressure drop in the real and test tubes. The major difference in the two-phase pressure drop compared to single-phase presented is that vapor quality and void fraction have to be taken into account in two-phase tests because these two parameters would affect the values of D_h and thus Re and friction factors. Equation (1) then must be modified accordingly to account for the influences of the two-phase phenomena so that the equivalent friction factor in two-phase flow can be accurately determined. In the two-phase region, steam vapor flows over the two-phase interface on the steel side and over the smooth polycarbonate surface on the visualization window as is illustrated in Figure 5(b), so f_{pc} is still the same as it is in the single-phase test but f_{st} needs to be replaced by the interfacial friction factor f_{int} that is a function of film thickness (Hewitt, 2013). Having the information of f_{int}, steam mass flux, and geometry of the full tube, the prediction of full tube pressure drop based on the test tube measurements then becomes feasible.

3.3 Model Validation

To verify the model in single phase, three independent experiments were conducted to measure friction factors in different tubes. The first experiment was in a full-sized flattened steel condenser tube with cross section shown in Figure 2, and the length for the pressure drop measurement section was 9.22 m. This full steel tube was made in the same way and by the same vendor as the one forming the test tube. The second experiment was in a rectangular polycarbonate duct with cross section 90.5 mm by 93.1 mm, and the length for the pressure drop measurement section was 1.13 m. This polycarbonate duct was made from the same material as the polycarbonate window in the half flattened condenser tube. The intention of using the same materials is to guarantee that the friction factor measured in these two experiments can accurately reproduce the friction factors on both the steel side and polycarbonate side in the test tube. The third experiment was in the test tube and the length for the pressure drop measurement section was 8.58 m. Due to the large interval volumes of the full and test tubes, high-pressure nitrogen gas was used in the test, while low-pressure compressed air was used in testing the polycarbonate tube because of its small size.

The friction factors, and therefore surface roughnesses, are determined in a slightly different manner for each tube. For the polycarbonate tube, where surface roughness is negligibly small, the friction factor is determined by Equation (5) that was derived from Prandtl's one-seventh power law (Prandtl, 1969).

$$f = 4 \times 0.078\, \mathrm{Re}_{D_h}^{-1/4} \quad (5)$$

Steel surface roughness is determined using Churchill's correlation (Equation (4)). For both tubes, surface roughness is determined in the turbulent and transition regions, where friction factor is a function of surface roughness.

To verify the accuracy of the determined friction factors, they were compared to several correlations based on flow regime. In fully-developed laminar flow inside rectangular ducts, Natarajan & Lakshmanan (1972) developed an equation to relate friction factor, Reynolds number and aspect ratio as shown in Equation (6).

$$f\, \mathrm{Re}_{D_h} = 4 \times 14.4 \alpha^{-1/6} \quad (6)$$

A number of turbulent friction factor correlations are available in literature such as those developed by Colebrook & White (1937) and Haaland (1983), which are shown in Equation (7) and (8). These turbulent models are implemented to verify the validity of Equation (1) through (3) with experimental results.

$$\frac{1}{\sqrt{f}} = -2 \log \left(\frac{\varepsilon}{3.7056 D_h} + \frac{2.5226}{\mathrm{Re}_{D_h} \sqrt{f}} \right) \quad (7)$$

$$\frac{1}{\sqrt{f}} = -1.8 \log \left[\left(\frac{\varepsilon}{3.7 D_h} \right)^{1.11} + \frac{6.9}{\mathrm{Re}_{D_h}} \right] \quad (8)$$

Figure 6 is the friction factor of steel determined in the first experiment. Back fitting the friction factor measurements in the turbulent region using Churchill's equation (Equation (4)), surface roughness of steel (ε_{st}) is found to be 0.8546 mm with a standard error of 0.0704 mm. The major sources of uncertainties involved in the determination of ε_{st} are from the low pressure drop measurements. At low Reynolds number, pressure drop was so small in the full steel tube that the instrument limit was nearly reached. Even in the fully turbulent region when Re was above 7000, pressure drop was still below 100 Pa. This reasoning can be further verified by the measurement done in the polycarbonate duct in which the measurement points matched the predictions very well as shown in Figure 7.

Figure 7 is the friction factors measured in the second experiment. Experimental data aligned very well with the predictions by Colebrook for different small values of surface roughness and by Prandtl. As is expected that the roughness of polycarbonate should be very small, the data validate the usage of smooth tube assumption when calculating pressure drop inside the polycarbonate tube.

Figure 8 shows the measured friction factor in the half flattened tube. The data were compared with the equivalent friction factor, f_e, derived from the analytical model (Equation (2)). f_{st} and f_{pc} are evaluated based on the surface roughness measurements in the first and second experiments, therefore f_e is independent from the third experiment. A very good match between prediction and experiment data is exhibited.

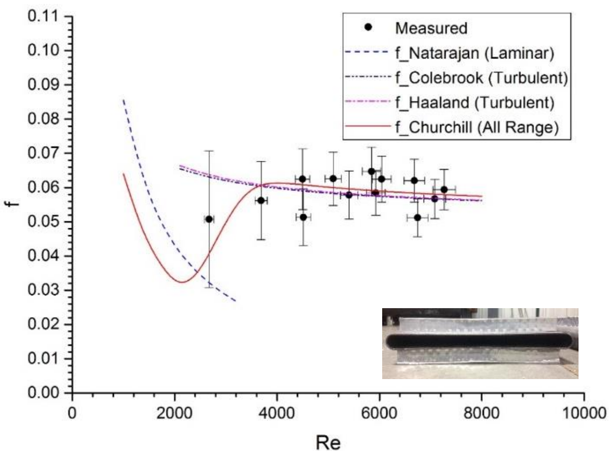

Figure 6: Comparison of Friction Factors in Steel Tube with Different Correlations

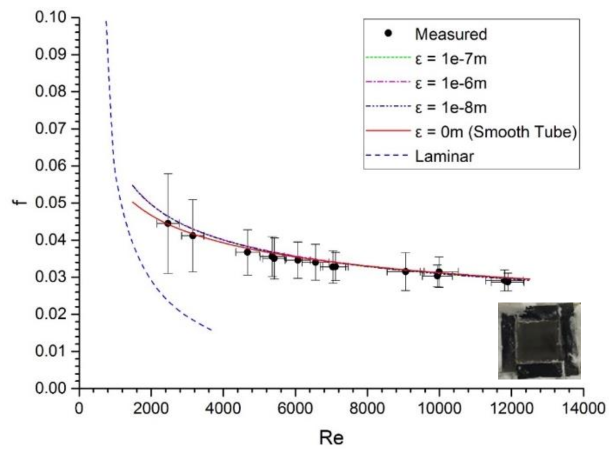

Figure 7: Comparison of Friction Factors in Polycarbonate Duct with Different Correlations

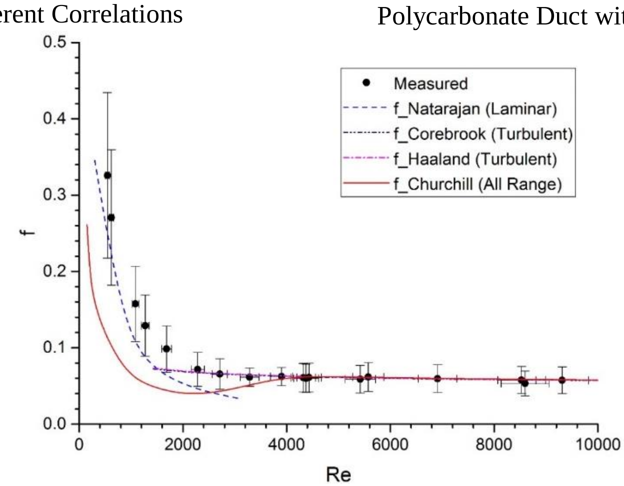

Figure 8: Comparison of Friction Factor in Test Tube with Different Correlations

Knowing the surface roughness of steel and polycarbonate from the first two experiments, the model successfully reproduced the pressure drop in the half tube within 5% error in turbulent region, and 40% error in low Reynolds number region compared with experimental data. Although the relative error of prediction is about 40% in laminar region, the absolute value of pressure drop inside the test tube is very small. Additionally, Churchill equation works for predicting pressure drop in all ranges of Reynolds number, but it was originally developed based on the round tube measurements. So the difference between Natarajan's and Churchill's predictions shown in Figure 6 to Figure 8 is justified, and experimental data fit Natarajan's correlation much better than Churchill's in the low Reynolds number region. Overall, the model in single-phase is proven to be a useful tool to relate test tube measurements to the full tube ones provided that the surface characteristics in both flattened tubes can be accurately determined. A modified two-phase model is under development and will be implemented to predict actual pressure drop performance in the ACC system in power plants.

4. EFFECT OF INCLINATION ON PRESSURE DROPS

4.1 Test Conditions

In-tube pressure drop was measured at various inclination angles. Limited by the ceiling height in the current laboratory setup, the test tube can only be inclined up to about 15˚. The preliminary test results were obtained under the conditions listed in Table 1. At different inclination angles, mass flow rate changes due to the changes in heat transfer inside the condenser tube. In order to account for the effects of different mass flow rate on pressure drop, boiler power was adjusted accordingly so that a constant flow rate condition can be maintained. The actual variation of mass flow rate at different inclination angles is less than 1.5%.

Table 1: Test Conditions

Parameter	Range	Uncertainty
Inlet vapor mass flux [kg m^{-2} s^{-1}]	6.8	$\pm$1
Mass flow rate of condensate [g s^{-1}]	10.0	$\pm$1
Condenser capacity [kW]	25.2 – 29.1	$\pm$3%
Air velocity (average) [m s^{-1}]	2.03	$\pm$7%
Vapor inlet pressure [kPa]	102 – 106	$\pm$0.1
Vapor inlet superheat [^{o}C]	0.1 – 0.7	$\pm$.05
Inclination angle [^{o}]	0.3 – 13.2	$\pm$0.4%

4.2 Results and Discussion

Figure 9 presents information about pressure measurements with error bars when the test tube was horizontal. Pressure drop per unit length was plotted to show the local pressure variation as a function of distance from the tube inlet. As is expected, pressure drop is much larger near the entrance of the test tube than it is near the exit due to the deceleration of steam vapor by condensation. In almost all measurements, the pressure drop in the first two-meter section is about half of the total pressure drop from inlet to the outlet. The gauge pressures at each individual pressure measurement point were also determined after knowing the inlet gauge pressure, atmospheric pressure and the pressure drop in each section.

In addition to the horizontal configuration, pressure variations along the tube at three other distinct inclination angles were shown in the same manner in Figure 10. No obvious effect of inclination angle on local pressure drop per unit length was observed within the range of angles tested. But the dependence of the total pressure drop from inlet to outlet on the inclination was discovered and is shown in Figure 11. Overall, the total pressure drop increased as inclination angle increased. The initial results showed an increase of 11.7% in pressure drop at 13.2 ^{o} versus at horizontal. However, there was a sudden decrease of total pressure drop at 2.87 ^{o}. This phenomenon can be explained by the initial visualization data shown in Figure 12, which presents the depth of condensate river along the tube at different inclination angles. The depth of condensate river gradually increased towards the exist of the test tube due to the accumulation of condensate downstream. The depth at each specific location decreased as the inclination angle increased. The increase in inclination angle assisted the drainage of condensate by gravity, which decreased the depth and thus increased the void fraction. So the gravity-assisted drainage exhibited a significant effect on pressure drop reduction when the depth dropped significantly at 2.87 ^{o} compared to the depth at horizontal.

Further investigation is underway to fully explore and understand the dependence of two-phase pressure drop on all ranges of inclination angles. The relationship between pressure drop and vapor mass flux, local vapor quality and void fraction will also be provided in the next stage of study.

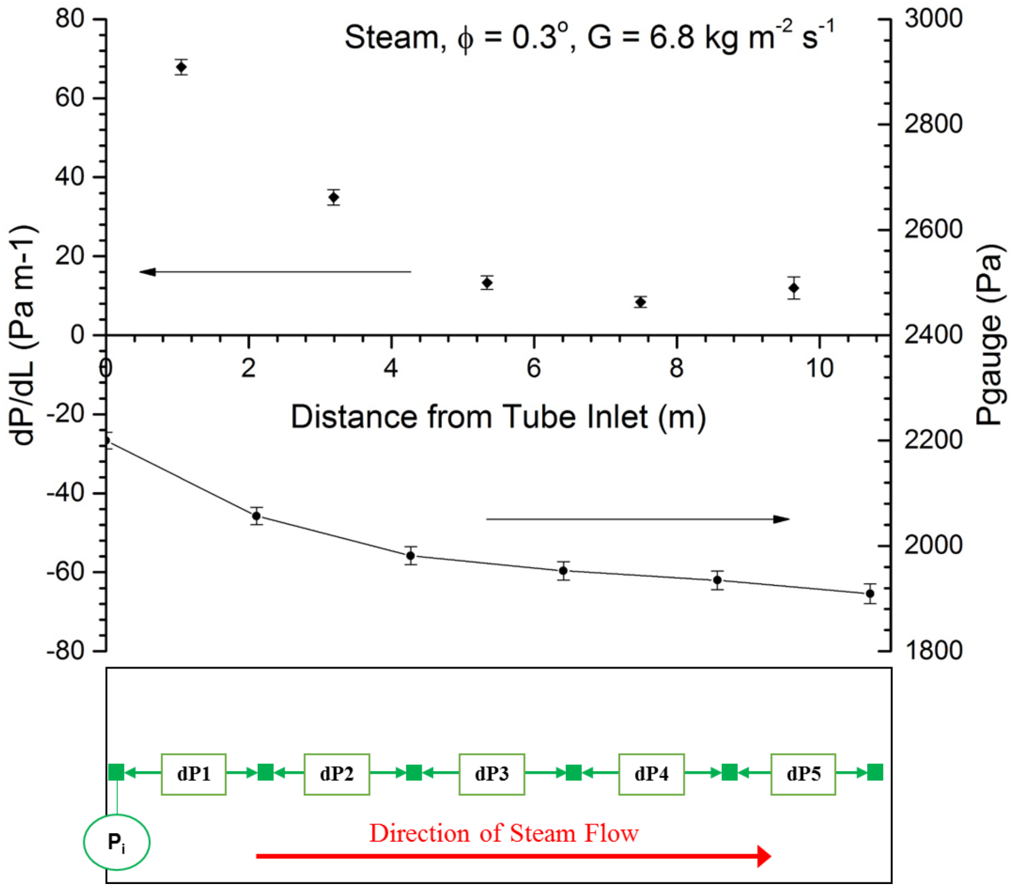

Figure 9: Pressure Variations Along the Tube at $\Phi = 0.3^{o}$

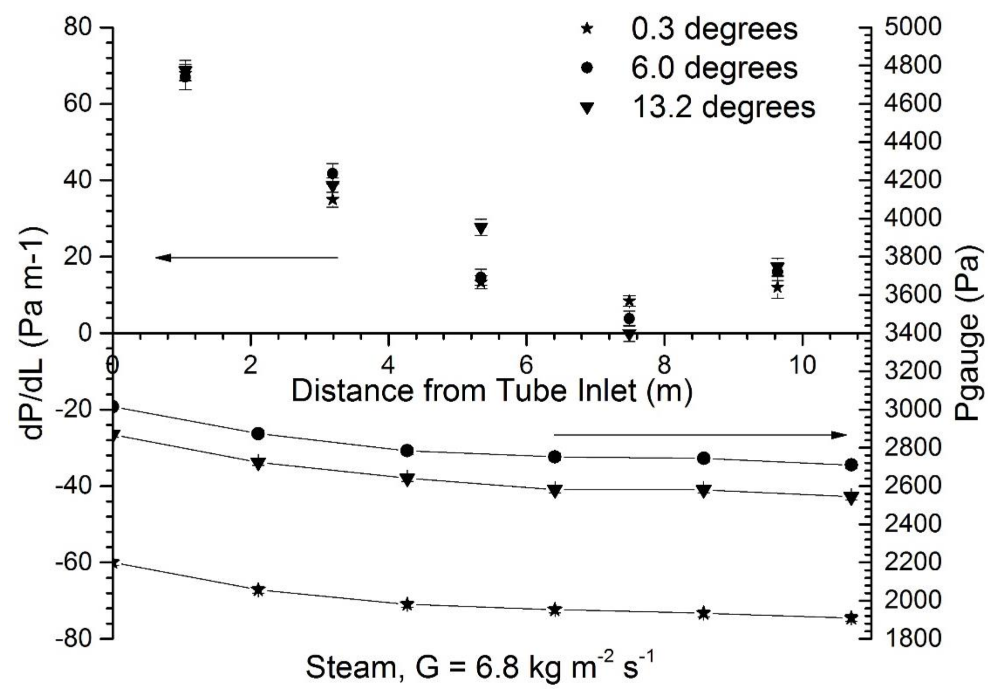

Figure 10: Pressure Variations Along the Tube at Different Inclination Angles

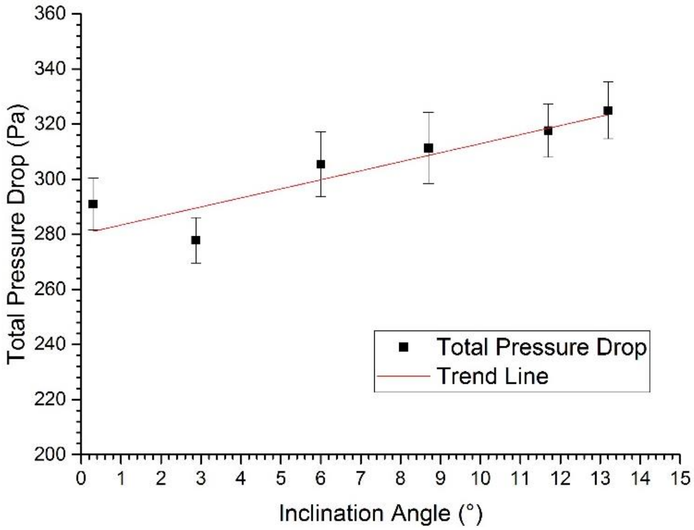

Figure 11: Total Pressure Drop at Different Inclination Angles

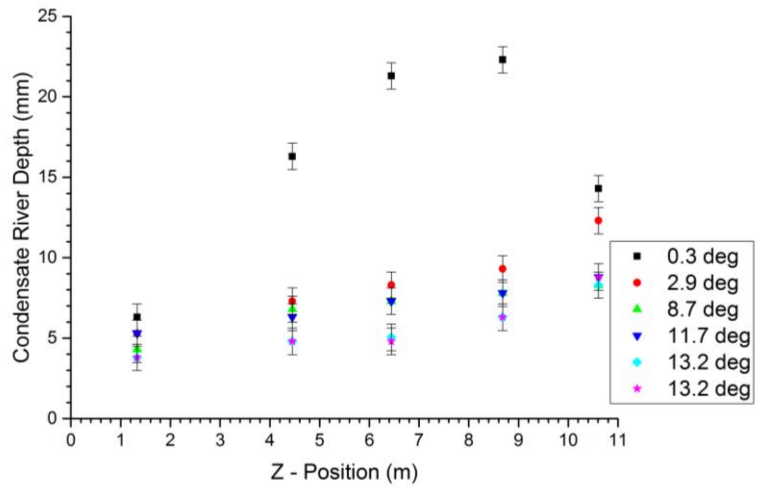

Figure 12: Depth of condensate river at discrete locations along the condenser

5. SUMMARY AND CONCLUSIONS

The experiment of steam condensation was conducted to research the effect of inclination on pressure drop. The inclination angle was varied from horizontal to 13.2^o with the intention of extending up to 90^o. Slightly superheated steam at the inlet was condensed in the 10.7 m long test tube at mass flow rate equal 10 g s^{-1}, resulting in mass flux of 6.8 kg m^{-2} s^{-1}. Pressure drop was measured and related to the inclination angles and flow visualizations. The issue resulting from the fact that the test tube was half of the real full size tube due to the need for visualization was mitigated by modeling pressure drop in single- and two-phase in both real and test tubes. Further development of the model for relating pressure drop is in progress. Based on the experimental results in this facility, it will provide a useful tool to predict two-phase pressure drop inside the condensers in the real power plants using ACCs.

The expected positive effect of inclination angle on the reduction of pressure drop due to gravity-assisted drainage of condensate has proven to be correct, although the effect only occurred at very early inclination stages. Further investigation into understanding this phenomenon is underway through the collection and interpretation of more data points in the next stage of research.

NOMENCLATURE

ACC	Air Cooled Condenser	
D	Diameter	(m)
ε	Surface Roughness	(mm)
f	Darcy Friction Factor	
G	Mass Flux	(kg m^{-2} s^{-1})
H	Height	(m)
L	Length	(m)
P	Pressure	(Pa)
p	Perimeter	(m)
Re	Reynolds Number	
T	Temperature	(˚C)
W	Width	(m)
ϕ	Angle of Inclination	(˚)

Subscript

a	Air
b	Bottom

e	Equivalent
h	Hydraulic
i	Inlet
int	Interface
o	Outlet
pc	Polycarbonate
s	Steam
sat	Saturation
st	Steel
t	Top
w	Wall

REFERENCE

Churchill, S. (1977). Friction factor equation spans all fluid flow regimes. *Chemical Engineering*, 91-92.

Colebrook, C., & White, C. (1937). Experiments with fluid friction in roughened pipes. *Proceedings of the Royal Society of London. Series A, Mathematical and Physical Sciences* , 367-381.

Coleman, J. W., & Garimella, S. (2003). Two-phase flow regimes in round, square and rectangular tubes during condensation of refrigerant R134a. *International Journal of Refrigeration*, 117-128.

Groenewald, W., & Kroger, D. (1995). Effect of mass transfer on turbulent friction during condensation inside ducts. *International Journal of Heat and Mass Transfer*, 3385-3392.

Haaland, S. (1983). Simple and explicit formulas for the friction factor in turbulent pipe flow. *Journal of Fluids Engineering*, 89-90.

Hewitt, G. (2013). *Annular Two-Phase Flow.* Elsevier.

Ide, H., & Matsumura, H. (1990). Frictional pressure drops of two-phase gas-liquid flow in rectangular channels. *Experimental Thermal and Fluid Science*, 362-372.

Kim, N., Lee, E., & Byun, H. (2013). Condensation heat transfer and pressure drop in flattened smooth tubes having different aspect ratios. *Experimental Thermal and Fluid Science*, 245-253.

Lee, H., & Lee, S. (2001). Pressure drop correlations for two-phase flow within horizontal rectangular channels with small heights. *International Journal of Multiphase Flow*, 783-796.

Lips, S., & Meyer, J. (2011). Two-phase flow in inclined tubes with specific reference to condensation: A review. *International Journal of Multiphase Flow*, 845-859.

Lips, S., & Meyer, J. (2012). Experimental study of convective condensation in an inclined smooth tube. Part II: Inclination effect on pressure drops and void fractions. *International Journal of Heat and Mass Transfer*, 405-412.

Natarajan, N., & Lakshmanan, S. (1972). Laminar flow in rectangular ducts: Prediction of velocity profiles and friction factor. *Indian Journal of Science and Technology*.

Prandtl, L. (1969). *Essentials of Fluid Dynamics.* London: Blackie & Son.

Wambsganss, M., Jendrzejczyk, J., France, D., & Obot, N. (1992). Frictional pressure gradients in two-phase flow in a small horizontal rectangular channel. *Experimental Thermal and Fluid Science*, 40-56.

ACKNOWLEDGEMENT

This material is based upon work supported by the National Science Foundation under Grant No. CBET 13-57992.The authors also thankfully acknowledge the financial support provided by Electric Power Research Institute (EPRI), and the technical support provided by the Air Conditioning and Refrigeration Center (ACRC) at University of Illinois at Urbana Champaign, and at the CTS - Creative Thermal Solutions, Inc.